Ryu *Nanoscale Research Letters* (2017) 12:366
DOI 10.1186/s11671-017-2141-6

Nanoscale Research Letters

NANO EXPRESS Open Access

Investigation into the Anomalous Temperature Characteristics of InGaN Double Quantum Well Blue Laser Diodes Using Numerical Simulation

Han-Youl Ryu

Abstract

GaN-based blue laser diodes (LDs) may exhibit anomalous temperature characteristics such as a very high characteristic temperature (T_0) or even negative T_0. In this work, temperature-dependent characteristics of GaN-based blue LDs with InGaN double quantum well (QW) structures were investigated using numerical simulations. The temperature-dependent threshold current is found to become increasingly anomalous as the thickness or doping concentration of the barrier layer between QWs increases. For a properly chosen barrier thickness and doping concentration, very high T_0 of >10,000 K can be obtained. The anomalous temperature characteristics of these InGaN blue LDs are attributed to the increase of gain at the n-side QW with increasing temperature because of the thermally enhanced hole transport from the p-side to the n-side QW.

Keywords: Characteristic temperature, GaN, Quantum well, Laser diode, Carrier transport

Background

Recently, GaN-based blue laser diodes (LDs) have attracted great attention for use in laser-based white lighting [1–3] and visible light communication applications [4–7]. The blue LD-based white light source can eliminate the "efficiency droop" problem, which has been commonly observed in GaN-based light-emitting diodes (LEDs) at high injection currents [1, 8–10]. In LDs, the carrier density in the active region is clamped at the lasing threshold, and the injected carriers above threshold are converted to photons by stimulated emission, without undergoing nonradiative recombination. This leads to increased power conversion efficiency with increasing injection current in blue LDs. Therefore, LD-based white light sources can be advantageous for high-power and high-brightness illumination.

For high-power lighting applications, thermally stable operation of blue LDs is highly desirable. The temperature dependence of LDs is generally described by the following empirical expression [11]:

$$I_{\mathrm{th}} = I_0 \exp(T/T_0), \tag{1}$$

where I_{th} and T are the threshold current and absolute temperature, respectively. I_0 is a constant having a dimension of current. T_0 is the characteristic temperature, a phenomenological parameter that represents the temperature dependence of LDs. High T_0 implies that I_{th} of LDs is less sensitive to the temperature change. If I_{th} is constant as temperature varies, T_0 will go to infinity.

Normally, the I_{th} of LDs increases with T because of various temperature-dependent mechanisms such as thermal broadening of the gain spectrum, thermally activated carrier escape, free-carrier absorption, and Auger recombination. Most of the reported T_0 values of GaN-based blue-violet LDs ranged from 120 to 180 K [12–15]. In some reports, however, anomalously high T_0 of >200 K or even negative T_0 values have been demonstrated [16–20]. Negative T_0 implies that I_{th} decreases with increasing temperature. Bojarska et al. reported that the T_0 of InGaN LDs increases as the emission wavelength increases owing to a reduction in

Correspondence: hanryu@inha.ac.kr
Department of Physics, Inha University, Incheon 402-751, South Korea

the thermal escape of electrons from quantum wells (QWs) with increasing well depth [19]. Recently, they also observed negative T_0 from a blue LD sample having a large distance between the electron-blocking layer (EBL) and the QWs, which was attributed to the thermal improvement of carrier injection efficiency [20]. Ryu et al. observed very high T_0 and negative T_0 in blue LD samples having double QWs [17, 18], which was ascribed to the thermally enhanced hole redistribution between the QWs. As the temperature increases, the carrier distribution in QWs become homogeneous, which is believed to increase gain in QWs and consequently decrease the lasing threshold. However, despite the experimental evidence of such anomalous temperature characteristics, thus far, the fundamental mechanism governing the value of T_0 has not been clearly identified.

Numerical simulations of LD device characteristics may give insight into the origin of the anomalous T_0 of InGaN blue LDs. In this paper, the temperature dependence of light output power as a function of injection current (*L-I*) in blue LD structures is numerically investigated using the simulation software, LASer Technology Integrated Program (LASTIP) [21]. LASTIP has been widely used in the study of semiconductor laser characteristics. In the present simulations, the active region is considered to be composed of InGaN double QW layers separated by a barrier layer. Since carrier transport and distribution in QWs is strongly influenced by the barrier layer between the QWs [18], the temperature dependence of the *L-I* curves is investigated as the thickness and doping concentration of the barrier layer are varied. In the next section, the simulated LD structure and the simulation method are described. In the "Results and Discussion" section, simulation results of various temperature characteristics are presented and the origin of the anomalous temperature characteristics in the InGaN blue LDs is discussed.

Methods

The LD structure for the simulation is basically similar to that reported in Ref. [18]. A schematic of the simulated LD structure is shown in Fig. 1a. The active region consists of two 2.5-nm $In_{0.15}Ga_{0.85}N$ QW layers separated by an $In_{0.02}Ga_{0.98}N$ barrier layer, which resulted in an emission wavelength of 449 nm. 1.2-μm n-$Al_{0.04}Ga_{0.96}N$ and 0.6-μm p-$Al_{0.05}Ga_{0.95}N$ layers are used as the bottom and the top cladding layer, respectively. A 20-nm p-$Al_{0.2}Ga_{0.8}N$ EBL layer is employed to suppress electron leakage from the active region to p-GaN. A background electron concentration of 1×10^{17} cm^{-3} is assumed in the unintentionally doped QW and barrier layers [22]. Figure 1b shows profiles of the refractive index and the wave intensity of the lasing mode when the barrier thickness is 10 nm as a function of vertical position. The origin of the vertical position corresponds to the bottom interface of the n-side QW as shown in Fig. 1. The refractive index data of GaN, AlGaN, and InGaN alloys at 450 nm were adopted from Ref. [23]. The LD layer structures were designed so that the optical mode was asymmetrically distributed as shown in Fig. 1b. This design is known to be advantageous in avoiding the catastrophic optical damage of the laser mirror facet [14, 24]. The optical confinement factor of the lasing mode was calculated to be 0.63%. The LD chip structure has the form of a narrow-stripe ridge waveguide with a ridge width of 2.6 μm and a cavity length of 650 μm. Power reflectivity on the front and rear facet is 56 and 95%, respectively.

LASTIP self-consistently solves QW band structures, radiative and nonradiative carrier recombination, the drift and diffusion equation of carriers, and photon rate equations. The built-in electric fields induced by spontaneous and piezoelectric polarizations at the hetero-interfaces, InGaN/GaN and AlGaN/GaN, are also included using the model described in Ref. [25], assuming 50% compensation of the polarization fields

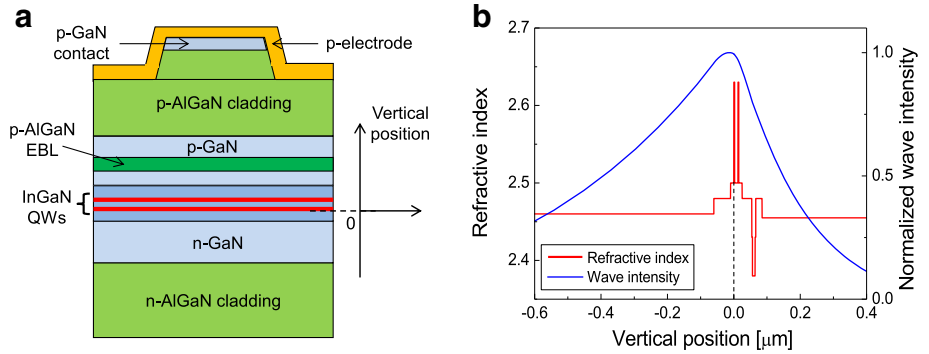

Fig. 1 **a** Schematic of the simulated LD structure. **b** Vertical profiles of the refractive index (*left vertical axis*) and the normalized wave intensity of the lasing mode (*right vertical axis*) of the simulated LD structure

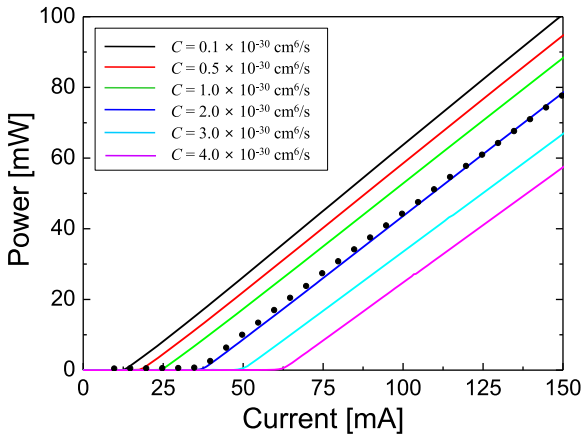

Fig. 2 *L-I* curves of the simulated LD structures for various Auger recombination coefficient (*C*) values from 1×10^{-31} to 4×10^{-30} cm^6/s at 20 °C. Here, the barrier thickness and doping concentration are fixed at 10 nm and 1×10^{17} cm^{-3}, respectively. The *L-I* curve of the reference LD is represented as *solid dots*

[26, 27]. The conduction band offset of $In_{0.15}Ga_{0.85}N/In_{0.02}Ga_{0.98}N$ active layers and AlGaN/GaN layers is set at 0.7 [10]. The Mg doping concentration of the p-GaN and p-AlGaN layers is fixed at 1×10^{19} cm^{-3}, and the Mg acceptor ionization energy is assumed to scale linearly from 170 meV (GaN) to 470 meV (AlN) [10, 28]. In the n-type doped layer, the electron concentration is assumed to be the same as the doping concentration. The mobility model in Refs. [29–31] was used for the mobility of carriers, which gave an electron mobility of ~500 cm^2/Vs for n-GaN with a doping concentration of 1×10^{18} cm^{-3}. The hole mobility in the AlGaN, InGaN, and GaN layers is assumed to be 5 cm^2/Vs [30].

In the carrier recombination model of LASTIP, the radiative recombination rate is calculated by integrating the spontaneous emission spectrum with a Lorentzian line-shape function. The Shockley-Read-Hall (SRH) recombination lifetime is assumed to be 20 ns. However, the effect of the SRH recombination on I_{th} was found to be almost negligible compared to the radiative or Auger recombination, if the SRH recombination lifetime is >10 ns. The *L-I* curve was found to depend strongly on the Auger recombination and the internal optical loss. The Auger recombination coefficient *C* and the internal loss η_i are chosen so that the simulated *L-I* curve can agree well with the measured one in Ref. [18]. The slope efficiency of the *L-I* curve is mainly determined by η_i. When η_i is 10 cm^{-1}, the slope efficiency is obtained to be ~0.7 W/A which corresponds fairly well to the measured slope efficiency of the reference LD structure in Ref. [18]. The internal loss of 10 cm^{-1} is also similar to that reported in InGaN blue LD structures [32, 33]. Figure 2 shows *L-I* curves for various *C* values from 1×10^{-31} to 4×10^{-30} cm^6/s at 20 °C when the barrier thickness is set at 10 nm and the barrier doping concentration is 1×10^{17} cm^{-3}. The *L-I* curve of the reference LD is plotted as solid dots [18]. As the coefficient *C* increases, I_{th} increases significantly, implying a strong influence of the Auger recombination on lasing threshold. When *C* is 2×10^{-30} cm^6/s, the simulated *L-I* curve agrees quite well with the measured *L-I* curve of the reference LD. Therefore, in the simulation of this work, *C* and η_i are fixed at 2×10^{-30} cm^6/s and 10 cm^{-1}, respectively.

Results and Discussion

In Fig. 3, the temperature dependences of *L-I* curves for different n-type doping concentrations of the barrier are compared when the barrier thickness is 10 nm. Figure 3a–c show simulated *L-I* curves for temperatures from 20 to 100 °C when the doping concentration of the barrier is 1×10^{17}, 2×10^{18}, and 3×10^{18} cm^{-3}, respectively. Figure 4 plots I_{th} as a function of temperature for barrier doping concentrations of 0.1, 1, 2, and 3×10^{18} cm^{-3}. When the doping concentration is 1×10^{17} cm^{-3}, a normal

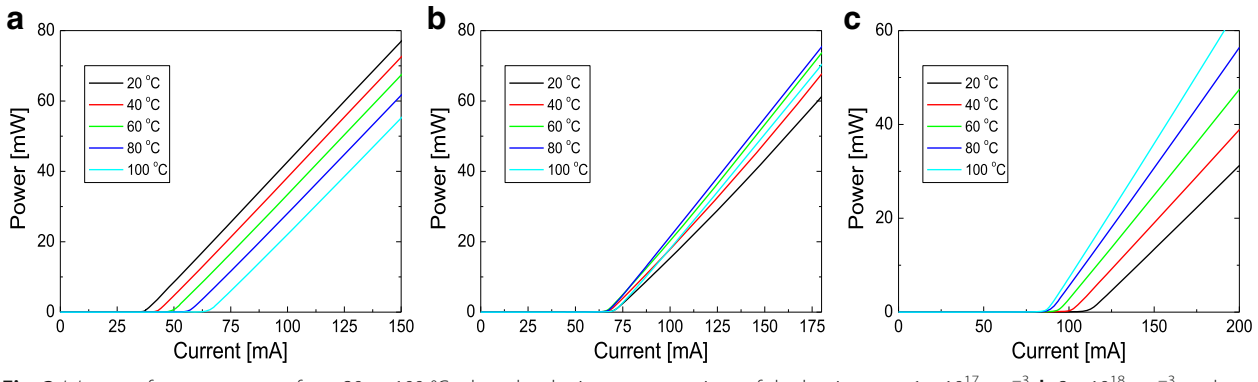

Fig. 3 *L-I* curves for temperatures from 20 to 100 °C when the doping concentrations of the barrier are **a** 1×10^{17} cm^{-3}, **b** 2×10^{18} cm^{-3}, and **c** 3×10^{18} cm^{-3}. Here, the barrier thickness is fixed at 10 nm

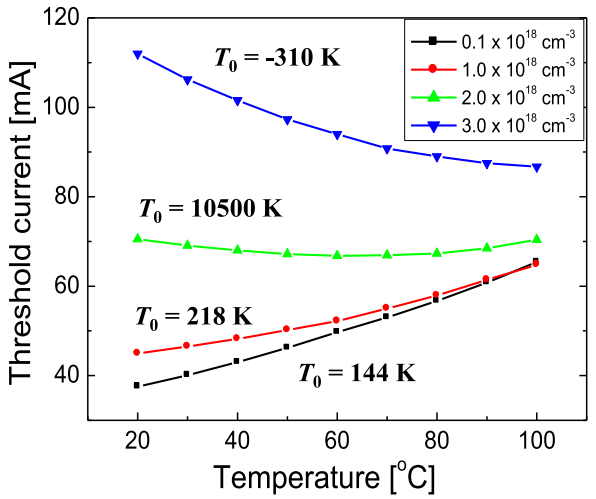

Fig. 4 Threshold current (I_{th}) as a function of temperature for barrier doping concentrations of 0.1, 1, 2, and 3×10^{18} cm^{-3}. The T_0 value for each doping concentration is shown. Here, the barrier thickness is fixed at 10 nm

temperature dependence of the *L-I* curves is observed. I_{th} increases steadily with temperature, resulting in a T_0 value of 144 K. For the doping concentrations of 2 and 3×10^{18} cm^{-3}, however, the temperature dependence of the *L-I* curves becomes anomalous. When the doping concentration is 2×10^{18} cm^{-3}, I_{th} is almost unchanged with increasing temperature, resulting in a very high T_0 of ~10,500 K. When the doping concentration is 3×10^{18} cm^{-3}, I_{th} decreases with temperature, therefore, a negative T_0 is obtained. This result indicates that the temperature dependence of I_{th} is strongly influenced by the doping concentration of the barrier layer in the InGaN blue LD structures. Figure 3b, c shows that the slope efficiency increases as the temperature increases, which has also been experimentally observed from a sample exhibiting negative T_0 in Ref. [20]. The reason for this increase will be discussed later. It should be noted that the anomalous temperature characteristics, very high or negative T_0, are accompanied by a substantial increase in the threshold current, which has also been observed experimentally [18, 20].

In order to understand the underlying mechanism related to the anomalous temperature characteristics, hole concentration and gain distribution in the QWs are calculated. Figure 5 shows the hole concentration distribution at 30 mA for temperatures of 20, 40, 60, and 80 °C when the n-type doping concentration of the barrier are (a) 1×10^{17} and (b) 2×10^{18} cm^{-3}. For the low doping case (1×10^{17} cm^{-3}), the hole concentrations of the two QWs are at a similar level and the hole distribution does not change significantly with temperature. For the high doping case (2×10^{18} cm^{-3}), however, the hole concentration of the n-side QW is much lower than that of the p-side one. This is because the n-type doping effectively increases the potential barrier height for holes, preventing the holes from transporting from the p-side to the n-side QW. As the temperature increases, the hole concentration at the n-side QW increases as a result of thermally enhanced hole carrier transport from the p-side to the n-side QW. Consequently, hole distribution in QWs becomes increasingly homogeneous as temperature increases. In comparison to the temperature-dependent hole concentration, it was found that the electron distribution at two QWs did not change significantly with temperature because of the much higher mobility of electrons.

Figure 6 shows the gain distribution below threshold at 30 mA for temperatures from 20 to 80 °C when the n-type doping concentration of the barrier are (a) 1×10^{17} and (b) 2×10^{18} cm^{-3}. For both doping concentrations, gain of the p-side QW is larger than that of the n-side QW, because of the higher carrier concentration at the p-side QW. For the low doping case (1×10^{17} cm^{-3}), gain at both QWs decreases as temperature increases. That is, the total gain decreases with increasing temperature mainly because of the thermal broadening of the gain spectrum

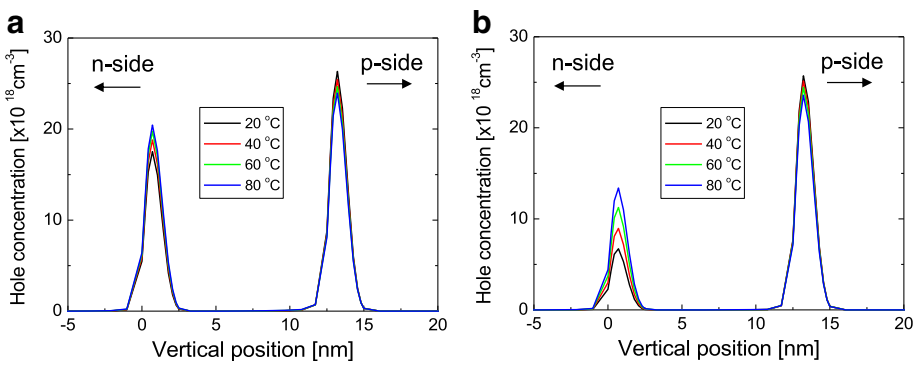

Fig. 5 Hole concentration distribution at 30 mA for temperatures of 20, 40, 60, and 80 °C when the n-type doping concentration of the barrier are **a** 1×10^{17} cm^{-3} and **b** 2×10^{18} cm^{-3}. Here, the barrier thickness is fixed at 10 nm

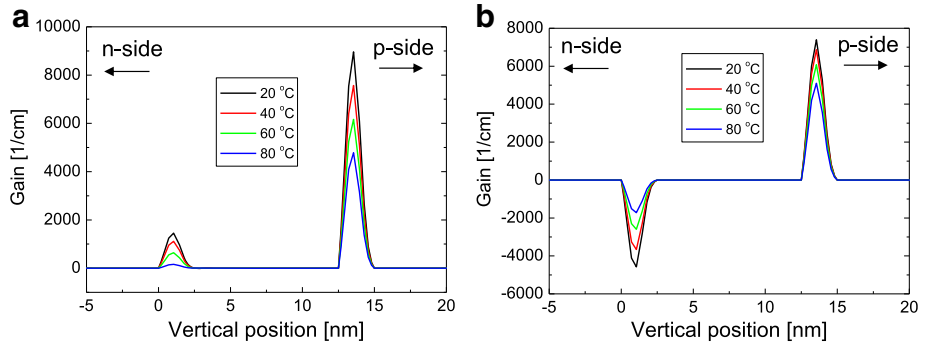

Fig. 6 Gain concentration distribution at 30 mA for temperatures of 20, 40, 60, and 80 °C when the n-type doping concentrations of the barrier are **a** 1×10^{17} cm^{-3} and **b** 2×10^{18} cm^{-3}. Here, the barrier thickness is fixed at 10 nm

[11]. As a result, I_{th} increased with temperature and normal temperature characteristics with T_0 of 144 K were obtained as shown in Fig. 3a. For the high doping case (2×10^{18} cm^{-3}), as temperature increases, gain at the n-side QW increases while gain at the p-side QW decreases. At the n-side QW, the increase of gain with increasing temperature results from the increase of the hole concentration with temperature as shown in Fig. 5b. In this case, the total gain changes only slightly with temperature, resulting in very high T_0 of >10,000 K, as shown in Fig. 3b. It should be noted that the gain at the n-side QW was negative over the entire temperature range. That is, the n-side QW absorbs light instead of amplifying it, which results in the increase of I_{th} and the decrease of slope efficiency. Since the absorption at the n-side QW decreases with temperature, the slope efficiency increases as the temperature increases, as observed in Fig. 3b.

When the barrier doping concentration was 3×10^{18} cm^{-3}, the total gain was found to increase with increasing temperature, resulting in the negative T_0. The simulation results of hole and gain distribution in Figs. 5 and 6 imply that the anomalous temperature characteristics (very high or negative T_0) of InGaN blue LDs are basically attributed to the thermal improvement of the hole injection efficiency from the p-side to the n-side QW layers.

Temperature-dependent characteristics are also investigated for other barrier thicknesses of 6 and 15 nm. Figure 7 plots the temperature dependence of I_{th} for a barrier thickness of (a) 6 and (b) 15 nm. When the barrier thickness is 6 nm, the temperature dependence of I_{th} is similar to that of when the doping concentration is from 1×10^{17} to 3×10^{18} cm^{-3} as shown in Fig. 7a. T_0 increases from 139 to 203 K as the doping concentration increases from 1×10^{17} to 3×10^{18} cm^{-3}. That is, the temperature dependence is basically normal for the entire simulation range of the doping concentration. This result implies that holes can transport efficiently from the p-side to the n-side QW even when the n-type doping concentration of the barrier is high if the barrier thickness is sufficiently thin.

When the barrier thickness is 15 nm, the temperature dependence of I_{th} becomes increasingly anomalous as the doping concentration increases. With this barrier

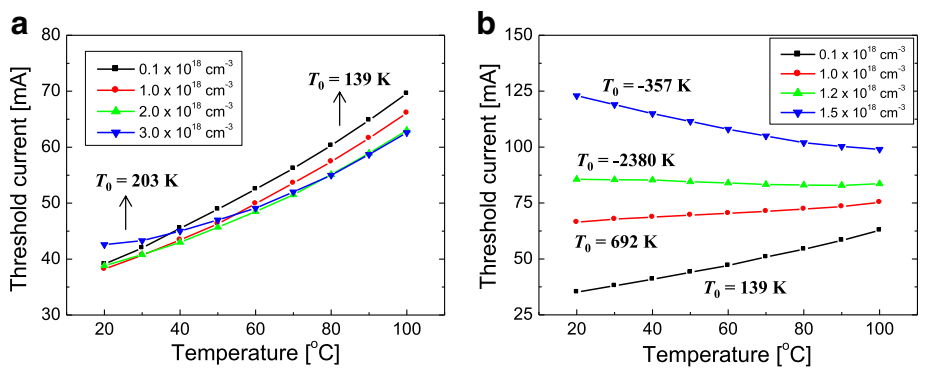

Fig. 7 Threshold current (I_{th}) as a function of temperature for barrier doping concentrations of 0.1, 1, 2, and 3×10^{18} cm^{-3} when the barrier thicknesses are **a** 6 and **b** 15 nm. The T_0 value for each doping concentration is shown. Here, the barrier doping concentration is fixed at 1×10^{18} cm^{-3}

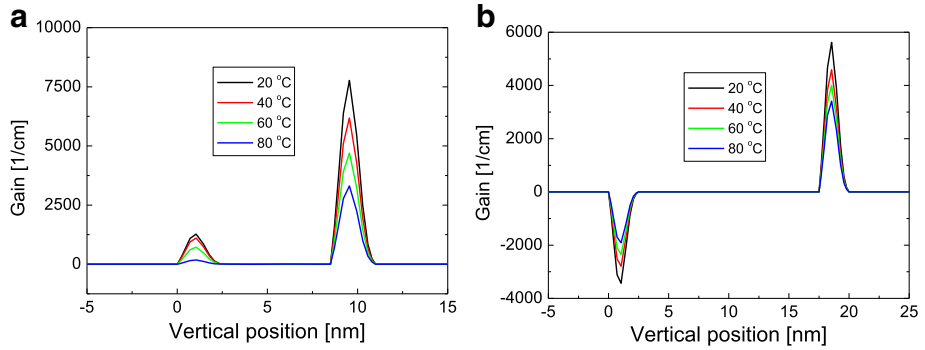

Fig. 8 Gain concentration distribution at 30 mA for temperatures of 20, 40, 60, and 80 °C when the barrier thicknesses are **a** 6 and **b** 15 nm. The T_0 value for each doping concentration is shown. Here, barrier doping concentration is fixed at 1×10^{18} cm^{-3}

thickness, the dependence of T_0 on doping concentration is more anomalous compared to that of when the barrier thickness is 10 nm. For the low doping case (1×10^{17} cm^{-3}), T_0 is almost the same for all three-barrier thicknesses: 6, 10, and 15 nm. However, when the doping concentration is increased to 1×10^{18} cm^{-3}, a high T_0 of 692 K is obtained. When the doping concentration is higher than 1.2×10^{18} cm^{-3}, a negative T_0 can be obtained. This result implies that holes have difficulty in transporting from the p-side to the n-side QW when the barrier is relatively thick.

Figure 8 shows temperature-dependent gain distribution at 30 mA for the barrier thicknesses of (a) 6 and (b) 15 nm when the doping concentration is 1×10^{18} cm^{-3}. When the thickness of the barrier is 6 nm, gain at both QWs is positive and decreases as temperature increases, which is similar to the result shown in Fig. 6a, where the barrier thickness is 10 nm and the doping concentration is 1×10^{17} cm^{-3}. When the barrier thickness is 15 nm, gain at the n-side QW is negative and increases with temperature, as similarly observed in Fig. 6b, where the barrier thickness is 10 nm and the doping concentration is 2×10^{18} cm^{-3}. This result implies that hole and gain distribution becomes increasingly inhomogeneous as the barrier thickness increases for a given doping concentration of the barrier. Consequently, the temperature characteristics become anomalous as the barrier thickness or doping concentration increases.

The anomalous temperature characteristics, very high or negative T_0, may be advantageous for some applications that require thermally stable LD operation. However, such anomalous temperature characteristics are often accompanied by a substantial increase in I_{th} and deterioration of device efficiency. However, with careful design of the active layer structure, InGaN blue LDs with high efficiency and temperature-stable operation are expected to be realized for potential use in LD-based solid-state lighting, display, and communication applications.

Conclusions

In this work, the temperature dependence of I_{th} in InGaN double QW blue LD structures was numerically investigated using the LASTIP simulator. Temperature dependent I_{th} and T_0 were found to depend strongly on the n-type doping concentration and the thickness of the barrier layer between QWs. T_0 was found to become increasingly anomalous as the thickness or doping concentration of the barrier layer between QWs was increased. When the barrier thickness was 10 nm and the doping concentration was 2×10^{18} cm^{-3}, a very high T_0 of >10,000 K was obtained. For a thicker barrier with higher doping concentration, negative T_0 was observed. From the simulation of carrier and gain distribution in the QWs, it was found that the anomalous temperature characteristics originate from the increase in the gain at the n-side QW with increasing temperature as a result of the thermal enhancement of the hole transport from the p-side to the n-side QW. The result of this work is also expected to be applied to designing AlGaAs- or InGaAsP-based LD structures for thermally stable operation.

Abbreviations

EBL: Electron-blocking layer; LASTIP: LASer Technology Integrated Program; LD: Laser diode; LED: Light-emitting diode; QW: Quantum well; SRH: Shockley-Read-Hall

Acknowledgements

This work was supported by the Nano Material Technology Development Program through the National Research Foundation of Korea (NRF) funded by the Ministry of Science, ICT and Future Planning (NRF-2015M3A7B7045490), and the Industrial Strategic Technology Developments Program (10052804) funded by the Ministry of Knowledge Economy, Korea Evaluation Institute of Industrial Technology (MKE/KEIT).

Author's Contributions

HYR wrote the manuscript and carried out all simulation works including the program coding, the structure design, and the execution of simulations.

Competing Interests

The author declares that he has no competing interests.

Publisher's Note

Received: 15 January 2017 Accepted: 12 May 2017
Published online: 19 May 2017

References

1. Wierer JJ, Tsao JY, Sizov DS (2013) Comparison between blue lasers and light-emitting diodes for future solid-state lighting. Laser Photonics Rev 7:963–993
2. Nakamura S (2015) Nobel lecture: background story of the invention of efficient blue InGaN light emitting diodes. Rev Mod Physics 87:1139–1151
3. George AF, Al-waisawy S, Wright JT, Jadwisienczak WM, Rahman F (2016) Laser-driven phosphor-converted white light source for solid-state illumination. Appl Optics 55:1899–1905
4. Watson S, Tan M, Najda SP, Perlin P, Leszczynski M, Targowaski G, Grzanka S, Kelly AE (2013) Visible light communications using a directly modulated 422 nm GaN laser diode. Opt Lett 38:3792–3794
5. Chi YC, Hsieh DH, Tsai CT, Chen HY, Kuo HC, Lin GR (2015) 450-nm GaN laser diode enables high-speed visible light communication with 9-Gbps QAM-OFDM. Opt Express 23:13051–13059
6. Lee C, Zhang C, Cantore M, Farrell RM, Oh SH, Margalith T, Speck JS, Nakamura S, Bowers JE, DenBaars SP (2015) 4 Gbps direct modulation of 450 nm GaN laser for high-speed visible light communication. Opt Express 23:16232–16237
7. Shen C, Ng TK, Leonard JT, Pourhashemi A, Oubei HM, Alias MS, Nakamura S, DenBaars SP, Speck JS, Alyamani AY, Eldesouki MM, Ooi BS (2016) High-modulation-efficiency, integrated waveguide modulator-laser diode at 448 nm. ACS Photonics 3:262–268
8. Pourhashemi A, Farrell RM, Hardy MT, Hsu PS, Kelchner KM, Speck JS, DenBaars SP, Nakamura S (2013) Pulsed high-power AlGaN-cladding-free blue laser diodes on semipolar (2021) GaN substrates. Appl Phys Lett 103:151112
9. Chow WW, Crawford MH (2015) Analysis of lasers as a solution to efficiency droop in solid-state lighting. Appl Phys Lett 107:141107
10. Piprek J (2016) Comparative efficiency analysis of GaN-based light-emitting diodes and laser diodes. Appl Phys Lett 109:021104
11. Coldren LA, Corzine SW (1995) Diode lasers and photonic integrated circuits. Wiley, New York
12. Asano T, Tojyo T, Mizuno T, Takeya M, Ikeda S, Shibuya K, Hino T, Uchida S, Ikeda M (2003) 100-mW kink-free blue-violet laser diodes with low aspect ratio. IEEE J Quantum Electron 39:135–140
13. Kozaki T, Matsumura H, Sugimoto Y, Nagahama S, Mukai T (2006) High-power and wide wavelength range GaN-based laser diodes. Proc SPIE 6133:613306
14. Ryu HY, Ha KH, Lee SN, Jang T, Son JK, Paek HS, Sung YJ, Kim HK, Kim KS, Nam OH, Park YJ, Shim JI (2007) High-performance blue InGaN laser diodes with single-quantum-well active layers. IEEE Photon Technol Lett 19:1717–1719
15. Kelchner KM, Farrell RM, Lin YD, Hsu PS, Hardy MT, Wu F, Cohen DA, Ohta H, Speck JS, Nakamura S, DenBaars SP (2010) Continuous-wave operation of pure blue AlGaN-cladding-free nonpolar InGaN/GaN laser diodes. Appl Phys Express 3:092103
16. Świetlik T, Franssen G, Wisniewski P, Krukowski S, Łepkowski SP, Marona L, Leszczynski M, Prystawko P, Grzegory I, Suski T, Porowski S, Perlin P, Czernecki R, Bering-Staniszewska A, Eliseev PG (2006) Anomalous temperature characteristics of single wide quantum well InGaN laser diode. Appl Phys Lett 88:071121
17. Ryu HY, Ha KH, Lee SN, Jang T, Kim HK, Chae JH, Kim KS, Choi KK, Son JK, Paek HS, Sung YJ, Sakong T, Nam OH, Park YJ (2006) Highly stable temperature characteristics of InGaN blue laser diodes. Appl Phys Lett 89:031122
18. Ryu HY, Ha KH (2008) Effect of active-layer structures on temperature characteristics of InGaN blue laser diodes. Opt Express 16:10849
19. Bojarska A, Goss J, Marona L, Kafar A, Stanczyk S, Makarowa I, Najda S, Targowski G, Suski T, Perlin P (2013) Emission wavelength dependence of characteristic temperature of InGaN laser diodes. Appl Phys Lett 103:071102
20. Bojarska A, Marona L, Makarowa I, Czernecki R, Leszczynski M, Suski T, Perlin P (2015) Negative-T_0 InGaN laser diodes and their degradation. Appl Phys Lett 106:171107
21. LASTIP by Crosslight Software Inc. (2009) http://www.crosslight.com
22. Feng MX, Liu JP, Zhang SM, Jiang DS, Li ZC, Li DY, Zhang LQ, Wang F, Wang H, Yang H (2013) Design consideration for GaN-based blue laser diodes with InGaN upper waveguide layer. IEEE J Selected Topics in Quantum Electron 19:1500705
23. Zhang LQ, Jiang DS, Zhu JJ, Zhao DG, Liu ZS, Zhang SM, Yang H (2009) Confinement factor and absorption loss of AlInGaN based laser diodes emitting from ultraviolet to green. J Appl Phys 105:023104
24. Ryu HY, Ha KH, Son JK, Paek HS, Sung YJ, Kim KS, Kim HK, Park YJ, Nam OH (2009) Comparison of output power of InGaN laser diodes for different Al compositions in the AlGaN n-cladding layer. J Appl Phys 105:103102
25. Fiorentini V, Bernardini F, Ambacher O (2002) Evidence for nonlinear macroscopic polarization in III-V nitride alloy heterostructures. Appl Phys Lett 80:1204–1206
26. Flory CA, Hasnain G (2001) Modeling of GaN optoelectronic devices and strain-induced piezoelectric effects. IEEE J Quantum Electron 37:244–253
27. Piprek J (2012) AlGaN polarization doping effects on the efficiency of blue LEDs. Proc SPIE 8262:82620E
28. Piprek J, Li S (2011) Electron leakage effects on GaN-based light-emitting diodes. Opt Quant Electron 42:89–95
29. Farahmand M, Garetto C, Bellotti E, Brennan KF, Goano M, Ghillino E, Ghione G, Albrecht JD, Ruden PP (2001) Monte Carlo simulation of electron transport in the III-nitride wurtzite phase materials system: binaries and ternaries. IEEE Trans Electron Devices 48:535–542
30. Piprek J (2003) Semiconductor optoelectronic devices. ch.9, Academic Press, San Diego
31. Chen JR, Wu YC, Ling SC, Ko TS, Lu TC, Kuo HC, Kuo YK, Wang SC (2010) Investigation of wavelength-dependent efficiency droop in InGaN light-emitting diodes. Appl Phys B 98:779–789
32. Ryu HY, Ha KH, Son JK, Lee SN, Paek HS, Jang T, Sung YJ, Kim KS, Kim HK, Park Y, Nam OH (2008) Determination of internal parameters in blue InGaN laser diodes by the measurement of cavity-length dependent characteristics. Appl Phys Lett 93:011105
33. Becerra DL, Kuritzky LY, Nedy J, Abbas AS, Pourhashemi A, Farrell RM, Cohen DA, DenBaars SP, Speck JS, Nakamura S (2016) Measurement and analysis of internal loss and injection efficiency for continuous-wave blue semipolar (2021) III-nitride laser diodes with chemically assisted ion beam etched facets. Appl Phys Lett 108:091106